Eur Phys J C **34**, s01, s403–s409 (2004)
Digital Object Identifier (DOI) 10.1140/epjcd/s2004-04-042-6

EPJ C direct
electronic only

Particle identification with the LHCb experiment

C. Jones

University of Cambridge, Madingley Road, Cambridge, CB3 0HE, e-mail: Christopher.Rob.Jones@cern.ch

Received: 26 June 2003 / Accepted: 9 February 2004 /
Published Online: 13 July 2004 –

Abstract. The status of the design and construction of the LHCb detector components associated with particle identification is presented in relation to the current re-optimisation of the overall experiment. The methods used to perform particle identification are briefly described and the overall performance is discussed with reference to example decay channels.

1 Introduction

LHCb is a dedicated b physics experiment being built at the Large Hadron Collider (LHC) at CERN, Geneva. The experiment will perform precision measurements of CP violation and studies of rare decays in the b hadron sector exploiting the high energies and prolific production rate of b hadrons at the LHC.

Particle identification is a crucial component of the LHCb experiment. The ability to distinguish leptons and hadrons in the final states of a variety of b hadron decays is essential for the LHCb physics program. Hadron identification is achieved in LHCb using Ring Imaging Cherenkov (RICH) detectors and will enable the experiment to distinguish hadronic CP violating channels from background processes, as well as providing kaon identification for flavour tagging. The calorimeter and muon system provide lepton identification capabilities essential for both the offline analysis of leptonic final states and clean triggering.

This article will briefly describe the particle identification systems in LHCb. The experiment has recently undergone a re-optimisation to reduce the total material budget and thus improve its reconstruction performance. The status of the design and construction of the sub-detectors related to particle identification will be described in relation to the general detector re-optimisation. Finally, the overall particle identification performance will be presented with reference to example decay channels.

2 Experimental overview

Figure 1 shows a non-bending (vertical) plane view of re-optimised LHCb detector. LHCb is a single arm spectrometer designed to exploit the fact that at high energies both the b and $\overline{\mathrm{b}}$ hadrons are often produced in the same forward direction. The experiment has a forward angular coverage of 15–300 mrad in the bending plane of the LHCb dipole magnet while the acceptance in the non-bending plane is 15–250 mrad. The main components of the design are a vertex detector, tracking stations (TT and T1-T3), a dipole magnet, the RICH detectors (RICH1 and RICH2), the electromagnetic and hadronic calorimeters and finally the muon chambers (M1-M5). A more complete overview of the experiment, tracking performance, trigger performance and physics reach can be found elsewhere in these conference proceedings [1,2,3,4,5].

Table 1. Characteristics of the LHCb RICH detectors

	Aerogel	C_4F_{10}	CF_4
n	1.03	1.0014	1.0005
θ_c^{max} /mrad	242	53	32
$\Delta\theta_c$ /mrad	1.82	1.26	0.59
N_{pe}	6.8	30.3	23.2
P_{tresh}^{pion} / GeV/c	0.6	2.6	4.4
P_{tresh}^{kaon} / GeV/c	2.0	9.3	15.6

3 RICH detectors

The required momentum coverage of the RICH detectors is illustrated in Fig. 2a using the two body decay $\mathrm{B_d^0} \to \pi^+\pi^-$ and the many body decay $\mathrm{B_s^0} \to \mathrm{D_s^+}\pi^+\pi^-\pi^-$. In order to distinguish the $\mathrm{B_d^0} \to \pi^+\pi^-$ decay from other two-body final states, excellent π-K separation is required for high momentum tracks; 10 % of tracks have momenta greater than 150 GeV/c. The identification of kaons from the accompanying b hadron in a given selected decay provides a clean mechanism for determining the charge of the primary b quark. Efficient identification of such kaons which typically have low momentum (Fig. 2b), together with good particle identification in high multiplicity decays such as $\mathrm{B_s^0} \to \mathrm{D_s^+}\pi^+\pi^-\pi^-$, defines the corresponding lower momentum limit to be of the order of 1 GeV/c.

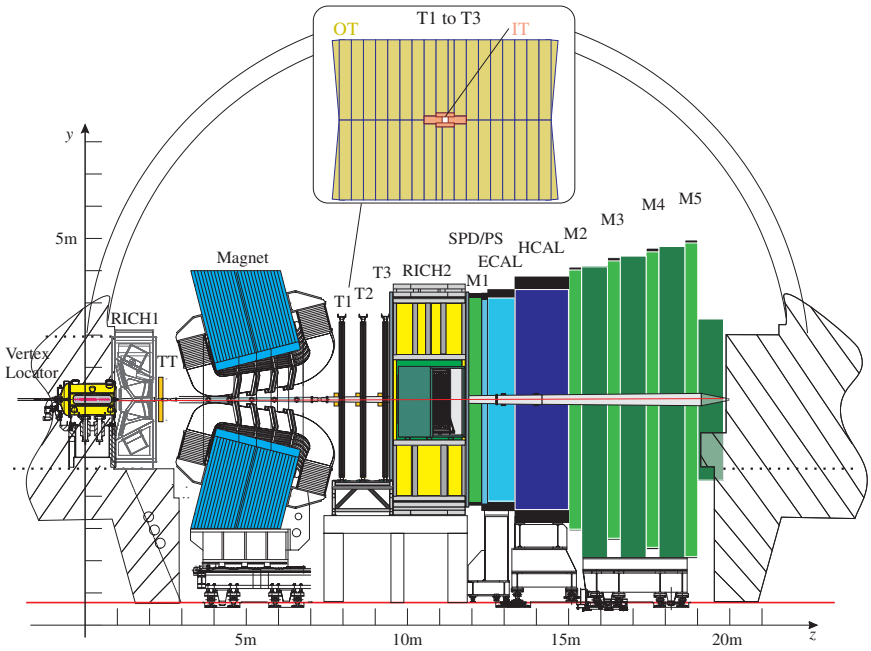

Fig. 1. The re-optimised LHCb detector viewed in the bending plane. The *upper figure* shows the inner (IT) and outer (OT) sub-components of the T1-T3 tracking stations

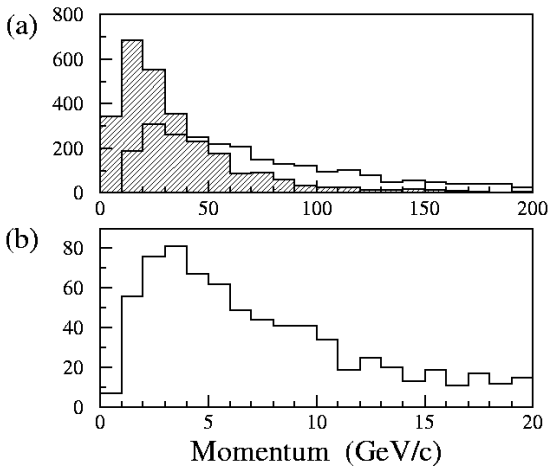

Fig. 2. a The momentum distribution for the highest momentum pion from $B^0_d \to \pi^+\pi^-$ (*unshaded*) and $B^0_s \to D^+_s\pi^+\pi^-\pi^-$ (*shaded*). **b** The momentum distribution for tagging kaons

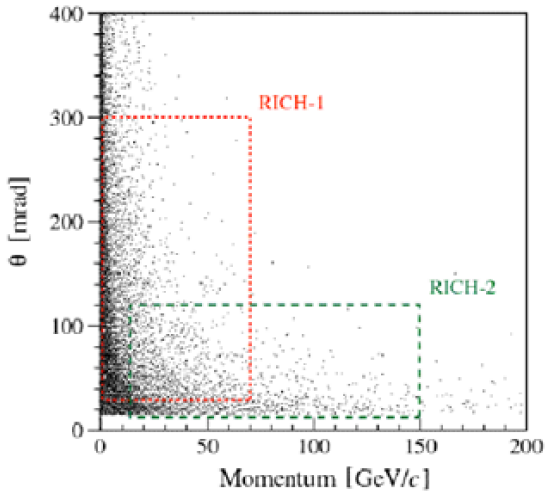

Fig. 3. Track polar angle versus momentum for $B^0_d \to \pi^+\pi^-$ decays. The acceptance of the RICH1 and RICH2 detectors are superimposed.

Figure 3 shows the correlation between the polar angle of a track traversing the spectrometer and its momentum. In order to satisfy the requirements of particle identification over a wide range of track momenta and polar angles, a ring imaging Cherenkov system was chosen consisting of 2 RICH detectors and utilising three radiator media with differing refractive indices.

RICH1 is placed close to the interaction point and covers track angles up to 300mrad using aerogel and gaseous C_4F_{10} radiators optimised for low to mid momentum tracks. RICH2 is placed further downstream, after the tracking systems and before the calorimeters and covers an acceptance out to 120mrad. Using a single radiator medium of gaseous CF_4 the detector is optimised for the higher momentum tracks. Table 1 details the physical parameters of the three radiators whilst Fig. 4 shows the Cherenkov angle versus momentum curves for each mass hypothesis.

The main optical components of each RICH detector are shown in Fig. 5. A traversing track radiates Cherenkov photons from the radiator media and these photons are both focused and brought out of the spectrometer acceptance using tilted spherical mirrors. Secondary flat mirrors

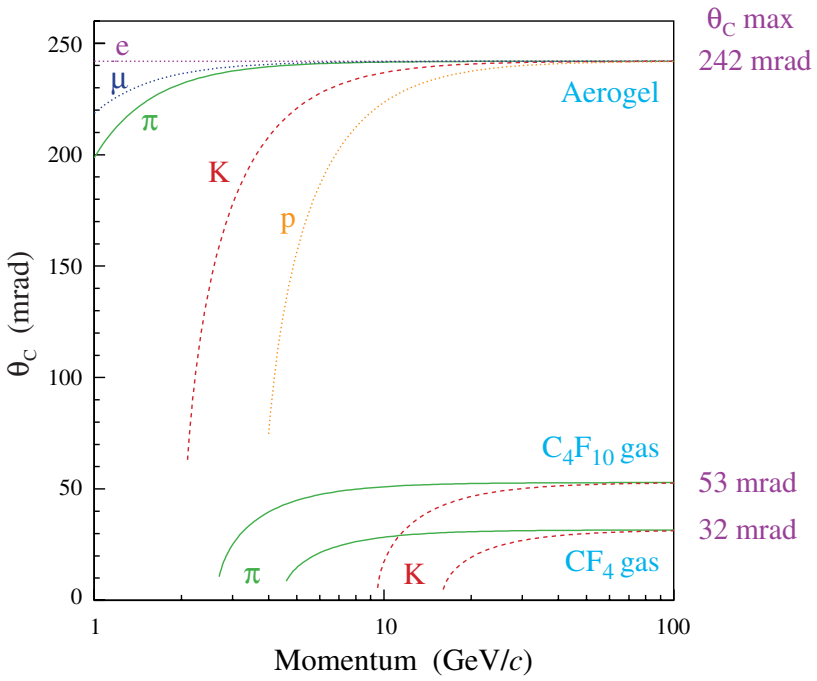

Fig. 4. The Cherenkov angle for the various mass hypotheses as a function of momentum

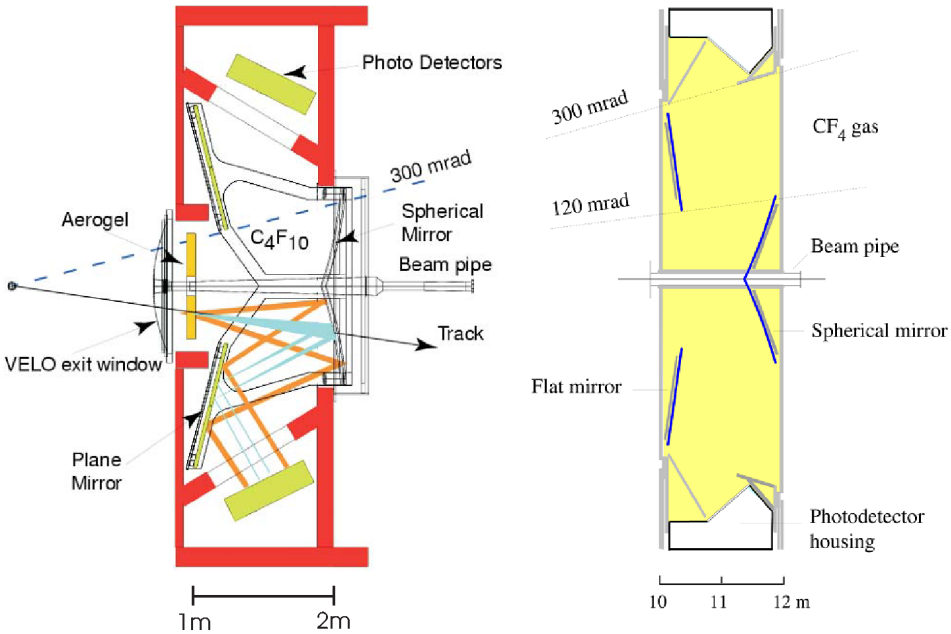

Fig. 5. Schematic views of the RICH1 (*left*) and RICH2 (*right*) detectors

are used to help bring the photons further out of the acceptance and also to allow the full length of the detector to be devoted to the gaseous radiator, resulting in a greater photon yield. Finally, photo-detectors are used to record and readout the signals.

3.1 RICH1

A primary aim of the LHCb re-optimisation program was to reduce the material in the spectrometer acceptance in order to improve the detector performance. RICH1 has been able to reduce its radiation length from 14 % to 8 %[1] and the interaction length from 4.5 % to 3.1 % without compromising the detector performance. These reductions has been achieved by introducing a variety of design modifications:

[1] Of which the radiator material contributes an irreducible 5.7 %.

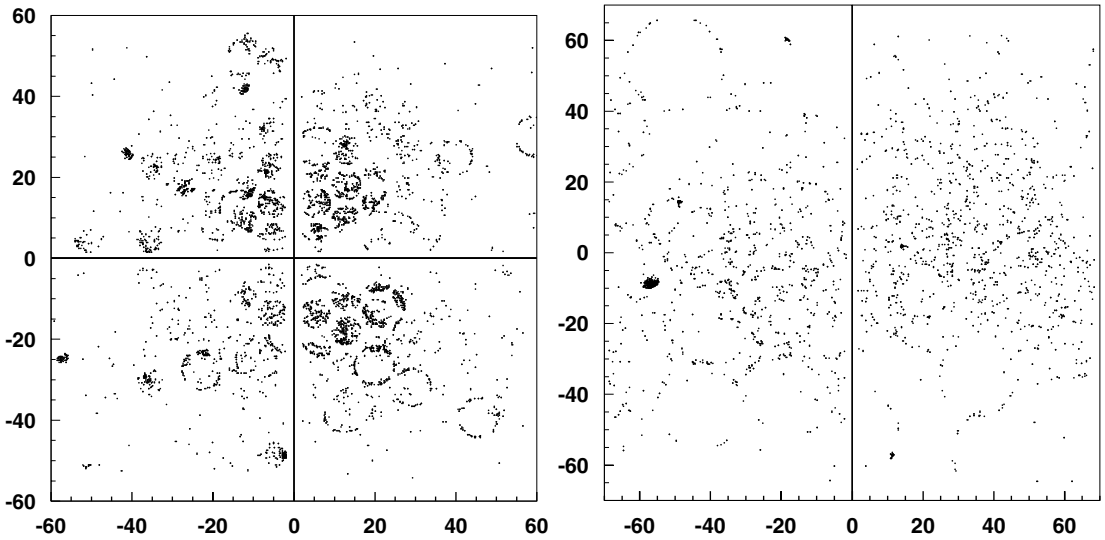

Fig. 6. A typical LHCb event as seen in RICH1 (*left*) and RICH2 (*right*). The photo-detector planes are drawn side-by-side for clarity

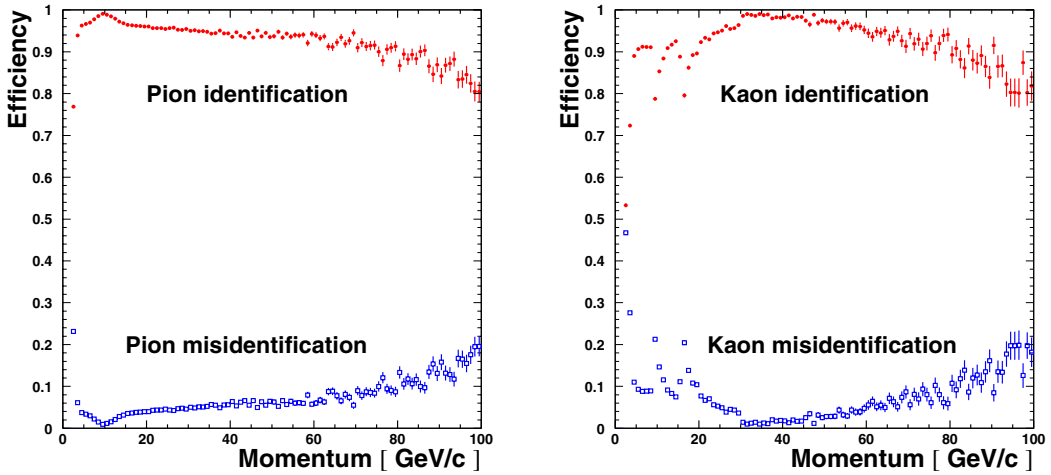

Fig. 7. Identification and mis-identification efficiencies for pions (*left*) and kaons (*right*). The dips in kaon performance at low momenta correspond to the thresholds in the three radiators

– The removal of the RICH1 entrance window and beam pipe seal. Instead, the detector will be sealed directly to the vertex detector vacuum tank.
– The use of light-weight material for the spherical mirrors. Prototype glass coated beryllium and carbon-fibre composites are under evaluation. Lighter mirrors also allow for reduced material in the mirror supports which can also be moved outside the spectrometer acceptance.

In addition, the trigger requirement for a fast momentum determination [5] requires that a magnetic field of the order of 500G be introduced in the vicinity of RICH1. Consequently the local shielding of the photo-detectors had to be significantly increased to reduce the fields at the photo-detectors to a satisfactory operating level. The new RICH1 design incorporates these constraints by:

– Using additional plane mirrors in order to allow the photo-detectors to be positioned further out of the acceptance such that extensive soft-iron shielding can be used.
– Changing the orientation of the detector from a horizontal arrangement to a vertical design. The original horizontal design would have required the introduction of large magnetic shielding boxes in the bending plane of the magnet, which would have reduced the field on axis in the very region it is required by the trigger.

The final details of the new RICH1 design are still under study, and a revised technical design will be presented in the LHCb re-optimisation TDR in September 2003.

3.2 RICH2

Due to its position downstream of the main LHCb spectrometer, the material budget of RICH2 is less critical

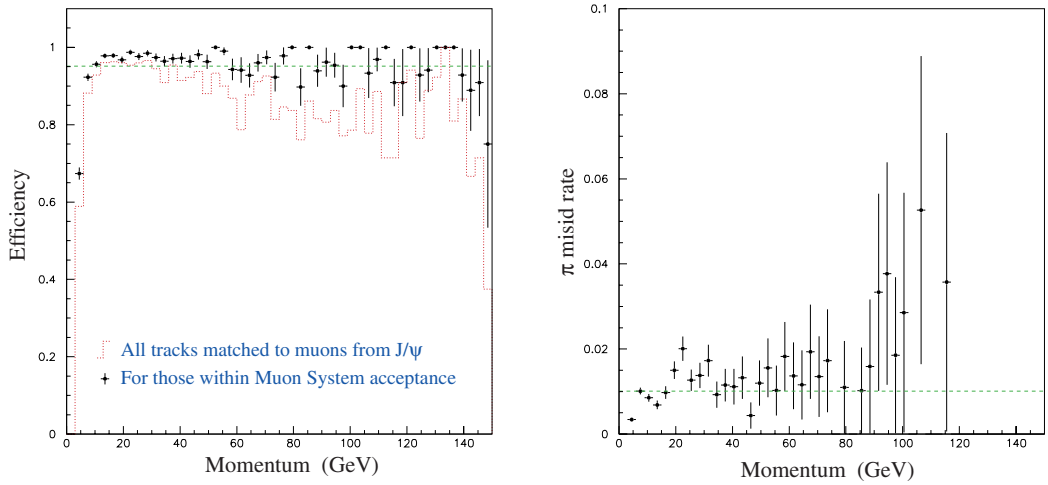

Fig. 8. The muon identification efficiencies (*left*) and mis-identification rates (*right*)

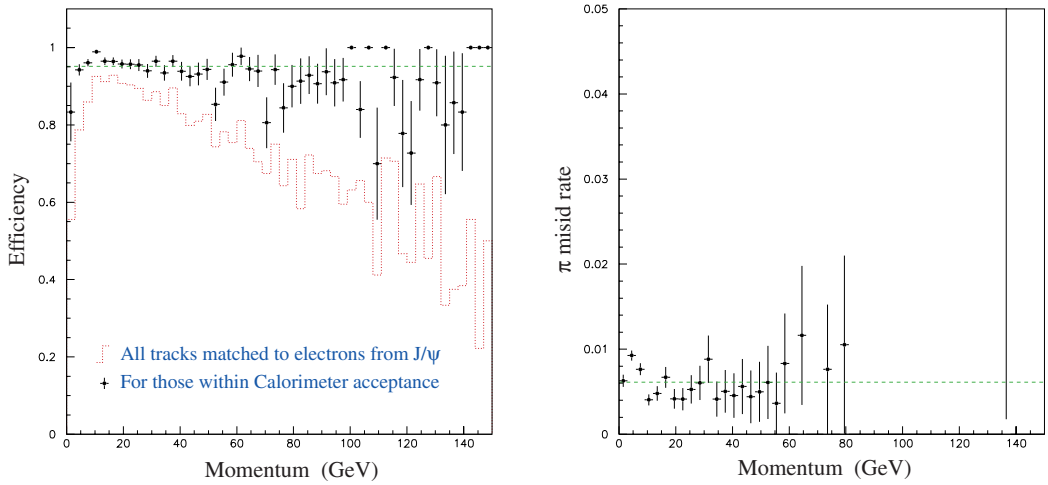

Fig. 9. The electron identification efficiencies (*left*) and mis-identification rates (*right*)

than in RICH1 and consequently the basic design of the detector has remained comparatively untouched by the LHCb re-optimisation process. The removal of tracking stations before RICH2 has however allowed for a 20 % increase in length of the CF_4 radiator medium. This increase in length leads directly to an enhanced Cherenkov photon yield and thus improved performance with respect to the design presented in the RICH TDR [6]. The final engineering design for RICH2 is progressing well with the Engineering Design Review approved in March 2002.

4 Hadron identification performance

The overall performance of the RICH system has been studied in full Geant simulations of LHCb events incorporating all known background sources and realistic reconstruction efficiencies. In addition, full pattern recognition in the tracking system is now available and thus the RICH performance has been evaluated in a fully realistic reconstruction environment which uses no reference to Monte Carlo information.

Figure 6, which shows a typical RICH event display illustrates the complex task evolved in RICH data analysis; only approximately 10 % of the hit pixels originate from primary tracks of interest. The current approach uses an implementation of a maximum-likelihood calculation to determine the most probable particle hypotheses. In this algorithm all available reconstructed trajectories through the RICH detectors, together with knowledge of the optics of the system, are used to predict the response of the photon detectors for a given choice of particle mass hypotheses. By comparing these predictions to the data the most likely set of mass hypotheses for all tracks is found. By considering all tracks simultaneously this "global" algorithm provides a complete description of the most important background contribution to a single Cherenkov ring, namely overlapping rings from neighbouring tracks.

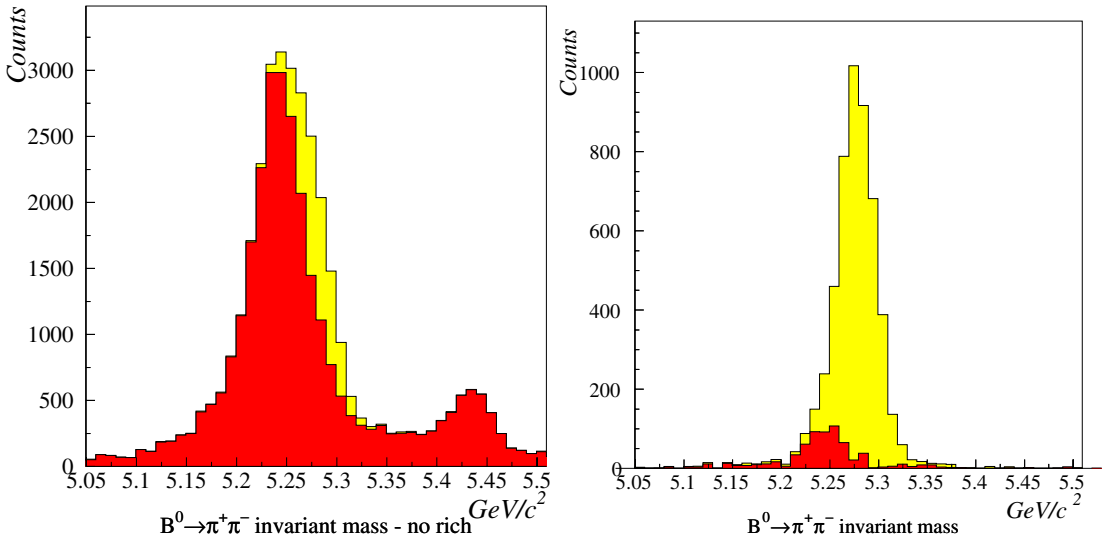

Fig. 10. The invariant mass distributions for $B^0_d \to \pi^+\pi^-$ decays without (*left*) and with (*right*) RICH particle identification information. The signal is shown by the light shaded region. All other topologically similar two body backgrounds are shown by the dark shaded region

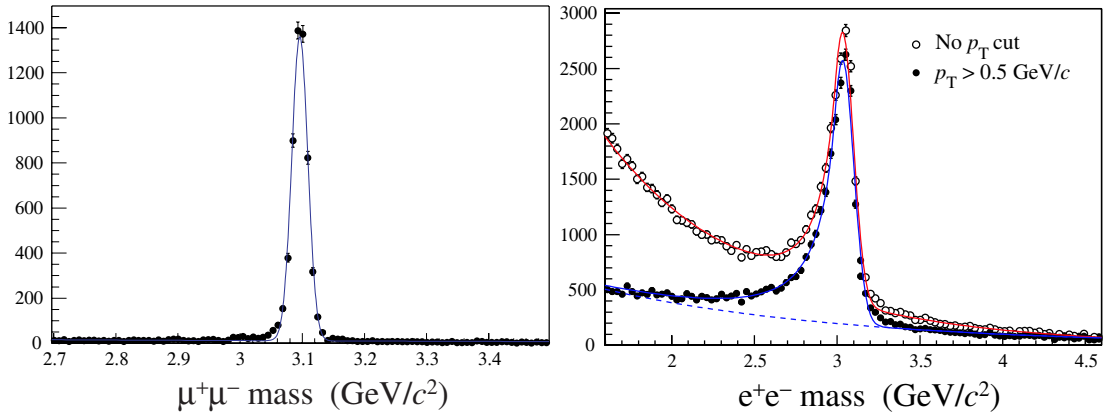

Fig. 11. Invariant mass for J/ψ reconstruction in $B^0_s \to (J/\psi \to l^+l^-)\,\phi$ decays

Alternative strategies are also being developed to compliment the global approach. These include a "local" approach which considers tracks individually and is therefore faster and less dependent on the overall tracking performance; and "Ring Finders" which attempt to isolate Cherenkov rings in the data without reference to reconstructed tracks. Studies into the optimal way to combine the information from the different approaches are continuing.

Figure 7 shows the pion and kaon selection performance as a function of reconstructed track momentum. Averaged over the full momentum range performance comparable to that presented in the TDR has been maintained, with pion and kaon efficiencies in excess of 90 % and mis-identification rates below 10 %.

5 Lepton identification performance

Both the calorimeter and muon system have had their respective TDRs [7,8] approved and are well advanced in their respective construction programs. Overall, the LHCb re-optimisation process has had minimal impact on the design of these sub-systems.

The muon system is based on multi-wire proportional chambers and particle identification is achieved by searching for hits in the detector chambers consistent with track projections from the spectrometer. A likelihood for the muon hypothesis is then built using a comparison of the separation and slope of the muon system hits to the projected track direction through the muon system. Figure 8 shows the excellent efficiency and purity of the muon selection obtained using this approach.

Electrons are identified using a combination of discriminating variables from the electromagnetic Shashlik calorimeter. For true electrons the electromagnetic cluster energy is comparable to the associated track momentum, whereas hadrons will deposit only a small fraction of their energy. The pre-shower detector also provides discrimination, where electrons are expected to produce a larger signal than hadrons. Figure 9 shows the resulting

efficiency and purity of an electron selection based on a combination of these discriminating variables.

6 Physics performance and conclusions

A full description of the performance of the re-optimised LHCb detector will be presented in detail in the TDR due in Autumn 2003. Figure 10 however, shows first results for the decay $B^0_d \to \pi^+\pi^-$ and clearly illustrates the importance of the RICH hadron identification. With excellent RICH hadron identification the purity of the selected $B^0_d \to \pi^+\pi^-$ decays is increased from 13 % to 84 % whilst retaining 79 % of the signal.

Figure 11 shows the invariant mass distributions for J/ψ reconstruction in $B^0_s \to (J/\psi \to l^+l^-)\,\phi$ decays. In the muonic channel, an efficiency of 86 % can be achieved whilst maintaining very low background levels. Efficient background rejection is more important for the electron channel, where without explicit rejection criteria a large combinatorial background from secondary electrons and ghost tracks is observed (Fig. 11b). However, by applying a $P_T > 0.5\,\mathrm{GeV/c}$ cut on the track transverse momentum an efficiency of 78 % is maintained whilst reducing background to a manageable level.

References

1. T. Nakada: 'LHCb Status', These Proceedings
2. M. Musy: 'LHCb Physics Reach', These Proceedings
3. J. van Tilburg: 'LHCb Tracking Performance', These Proceedings
4. A. Satta: 'LHCb: L0 Trigger and Related Detectors', These Proceedings
5. T. Schietinger: 'LHCb: L1 Trigger', These Proceedings
6. S. Amato et al., LHCb Collaboration: 'LHCb RICH: Technical Design Report' CERN-LHCC-2000-037
7. S. Amato et al., LHCb Collaboration: 'LHCb Calorimeters: Technical Design Report' CERN-LHCC-2000-036
8. S. Amato et al., LHCb Collaboration: 'LHCb Muon: Technical Design Report' CERN-LHCC-2001-010. Appendum CERN-LHCC-2003-002